Elucidating pore chemistry within Metal-Organic Frameworks via Single Crystal X-Ray Diffraction; from fundamental understanding to application.

Jorge Albalad,*[a] Christopher J. Sumby,[a] Daniel Maspoch*[b,c] and Christian J. Doonan*[a]

Metal-Organic Frameworks (MOFs) have made inroads in diverse chemical sectors due to the essentially limitless combination of building units and the ability to post-synthetically modify their pore chemistry at the molecular level. The crystalline nature of MOFs permits the use of Single Crystal X-Ray Diffraction (SCXRD) to obtain crystallographic snapshots of these transformations, providing invaluable information into the unorthodox chemistry that MOFs can potentially offer. This highlight article aims to provide the reader with the most recent milestones in the use of SCXRD as a vanguard technique to connect molecular-level pore engineering of MOFs with new application fields hitherto unexplored.

1. Introduction

Metal-Organic Frameworks (MOFs) are a class of solid-state materials that are poised for application in diverse industrial sectors.[1–4] MOFs are assembled via a bottom-up approach by linking metallic clusters, or cations, and multitopic organic building blocks together into an extended network. Indeed, the expansive variety of available inorganic nodes and organic units gives rise to an essentially limitless range of topologies and physical properties.[5] Furthermore, MOFs are typically microporous and retain their structures upon removal of internal guest molecules.[6,7] This unique collection of properties has encouraged researchers to explore MOFs for application to catalysis,[8] molecular separations,[9,10] gas sorption[11–13] and drug delivery.[14,15]

The modular approach to MOF synthesis affords the opportunity to synthesize solid-state materials with bespoke performance characteristics as the building-units provide chemical functionality representative of their molecular counterparts.[16] Additionally, MOF structures can be selectively modified under mild conditions by a strategy known as Post Synthetic Modification (PSM).[17] The technique of PSM has become increasingly widespread and we encourage readers interested in the development of this area to consult reviews dedicated to this topic.[18–22] A remarkable feature of PSM is that it allows for molecularly-precise engineering of the MOF pore chemistry, and thus the materials properties, while, typically, leaving the underlying scaffold unaffected.[23] Although researchers have extensively explored PSM of MOFs, molecular-level insight into this chemistry remains challenging.[24] For example, many spectroscopic characterisation techniques such as Induced Coupled Plasma (ICP), Mass Spectrometry (MS), or some Nuclear Magnetic Resonance (NMR) experiments are destructive and thus do not provide *in situ* information.[25] However, given that most MOFs are highly crystalline, Single-Crystal X-Ray Diffraction (SCXRD) is a powerful, non-destructive, tool for elucidating atomically-precise snapshots of MOF structures and providing global structural information such as framework topology and chemical functionality.[26] In addition, SCXRD can be used to identify the absolute configuration of entrapped molecular entities within the frameworks' lattice, including solution and gas-phase guests.[27] In summary, SCXRD has been a crucial technique to developing our fundamental understanding of MOF chemistry,[28] and will underpin future technological advancements in the field.

This article aims to highlight the importance of SCXRD as a tool for characterising MOF chemistry and advancing new applications of MOFs by canvassing selected milestones in the field. We begin by exploring how MOFs can be used as crystalline matrices for structurally identifying and exploring the reactivity of pore guests, as illustrated by the *Crystalline Sponge* method developed by Fujita *et. al.* We then look at how SCXRD can be used to identify physical adsorption processes in MOFs focusing on the interactions of small gas-phase molecules and the framework structure. Finally, we will cover how SCXRD is crucial to providing *in situ* insight into PSM chemistry and MOF-based catalysts. The examples in this manuscript were chosen because they provide significant insights into sample preparation/manipulation techniques. While this step is usually omitted from highlight articles, a proper handling of single-crystalline MOF samples is essential for obtaining the best diffraction quality and we hope will be useful for researchers interested in pursuing such chemistry. This highlight article is not intended to be an exhaustive review, rather to point the reader towards examples which exemplify the importance of SCXRD to the development of MOF chemistry. Further, we hope to give the reader an appreciation of how the information gathered from subtle structural insights, unobtainable by bulk characterisation techniques, will enable new areas of fundamental MOF research and facilitate practical applications.

2. The *Crystalline Sponge* method: MOFs as nanoscale molecular flasks

[a] *Department of Chemistry and Centre for Advanced Nanomaterials, The University of Adelaide, Adelaide, Australia. Email: jorge.albalad@adelaide.edu.au; christian.doonan@adelaide.edu.au.*

[b] *Catalan Institute of Nanoscience and Nanotechnology (ICN2), CSIC and Barcelona Institute of Science and Technology, Bellaterra 08193, Barcelona, Spain. Email: daniel.maspoch@icn2.cat.*

[c] *ICREA, 08010 Barcelona, Spain*

In 2010, Fujita's group introduced the *Crystalline Sponge* method,[29] which employs both discrete and extended porous materials as Crystalline Molecular Flasks (CMFs) to occlude and structurally characterise liquid guests by SCXRD.[30,31] A feature of CMFs is that their framework architectures are flexible, and thus accommodate structural rearrangements of their guests while maintaining crystallinity.[32,33] Since the first report of CMFs, Fujita and co-workers continued to develop the technique,[34] designing guest-selective CMFs for the SCXRD elucidation of chiral natural products,[35–39] volatile substrates,[40,41] chiral molecules,[42,43] and even to track *in situ* chemical transformations.[44] In these examples, the experimental parameters (*i.e.* guest solution concentration, temperature, incubation time, solvent) were carefully optimised, and were critical to ensure the highest encapsulation efficiency on each CMF system without losing crystallinity.

The first CMF systems had clear limitations, including structural fragility, incompatibility with polar/aqueous media, and moderate levels of guest encapsulation.[45] However, researchers have developed alternative protocols that overcome these restrictions. As a result, the *Crystalline Sponge* method has advanced from niche academic interest to showing potential use in industrial analytical chemistry,[46,47] becoming a reliable technique to determine the absolute configuration of important substrates which are difficult to crystallise on their own.

Recently, more sophisticated CMF systems have been designed in an effort to make the *crystalline sponge* method compatible with polar solvents. As an example, in 2019 de Gelder and co-workers developed a new family of water-stable lanthanide MOFs (RUM-1 to -3) that behave as promising and robust alternative hosts to allow application of the *Crystalline Sponge* method in polar media. These materials demonstrated long-term stability in a wide range of polar, protic, and coordinating solvents, unlike Fujita's counterparts, and were able to accommodate both hydrophobic and hydrophilic guests alike.[48]

The field of CMFs has matured significantly since its introduction *ca.* ten years ago. Behind the simple idea of trapping liquid substrates within nanoscale sponges lies a beautiful complexity of host-guest chemistry, preorganisation and structural design that permits to capture the interaction between CMFs and occluded substrates by SCXRD. Although the field still has some limitations, the *Crystalline Sponge* method has emerged as a very important tool for the structural analysis of trace compounds, *in situ* detection of reaction intermediates and to resolve the absolute configuration of natural and chiral products.[49] While not entirely alike, the *Coordinative Alignment* method presented by Yaghi and coworkers shares important points with the *Crystalline Sponge,* and precisely represents the level of structural information that can be gathered from interactions (in this case, covalent bonds) between host frameworks and guests.[50] It is anticipated that SCXRD will continue to drive advances in this area and be integral to facilitating its adoption in commercial analytical chemistry.[51]

3. Characterisation of gas-phase adsorption isotherms in MOFs via SCXRD

Understanding how gas-phase molecules interact with different parts of a framework has proven fundamental in the design of MOF-based adsorbent materials for potential application in industrial-scale adsorption and separation processes.[52,53] Initially, SCXRD was mainly used to identify preferential adsorption sites in as-synthesised MOF structures.[54,55] This study significantly advanced our understanding of the chemistry underpinning physisorption

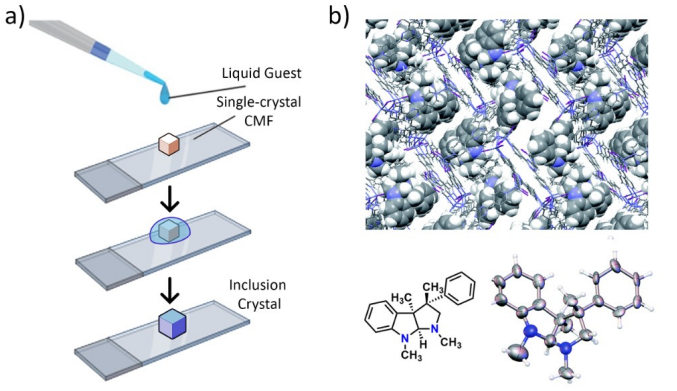

Figure 1. (a) Schematic for the preparation of a guest-included CMFs via the *Crystalline Sponge* method: a single-crystal piece of a CMF is treated with a drop of liquid guest and subjected to X-Ray data collection after incubation. (b) Absolute structure determination of a liquid guest by SCXRD (ORTEP drawing at 30% probability level) using the *Crystalline Sponge* method. Reproduced with permission of Reference 42.

steps in MOFs.[56,57] However, most of these early studies did not consider stimuli-responsive structural transitions.[58] Indeed, flexible MOFs can show drastic structural changes between their as-synthesised (solvated), activated, and gas-filled phases,[59] which has led to the discovery of unique properties such as MOF breathing,[60,61] gate opening,[62–64] hysteresis,[65–67] and more recently negative gas adsorption.[68–71] Because of the rapid nature of these transitions, their structural transformations during gas uptake are characterised by in situ high resolution X-ray and neutron diffraction, in combination with computational simulations[72,73] or NMR spectroscopy.[74] Though the collection times required for SCXRD are commonly incompatible with these steps the collection of initial (closed pore) and final (open pore) structures is crucial for obtaining atomically-precise models for theoretical calculations.[75]

Very few examples have been able to capture SCXRD snapshots of the critical inflexion points, such as intermediate loading stages, or hysteretic desorption steps. In 2019, Barbour et al. reported a molecular-level, SCXRD-based study of the hysteresis breathing behaviour of an interpenetrated Zn (II)-based MOF (**1**) responding to CO_2 gas pressure. In this work, the authors obtained crystallographic evidence of intermediate states of the adsorption-desorption cycle, as well as structural data of the interactions between CO_2 molecules within the framework, by using an environmental gas cell during *in situ* data collection. Complete crystallographic characterisation facilitated the rationalisation of each phase transformation during the slowly-triggered adsorption cycle, thereby providing a molecular-level explanation for the plateau observed during the desorption isotherm.[76]

The majority of SCXRD adsorption studies between MOFs and gas-phase guests are based on CO_2[53,77–79] and H_2O[80–82] interactions due to their strong binding affinities. Thus, these molecules give rise to more ordered structures compared to weakly-coordinating gas-phase substrates such as N_2, CH_4, O_2 or Ar. Accordingly, while there is a large collection of SCXRD data on the former, there is a paucity of data on the latter, which have remained widely ignored.[83,84] Not only do such weakly-coordinating guests exhibit disordered electron-density profiles around adsorption sites, but also face non-negligible competition from environmental H_2O during SCXRD data collection.[85] To overcome this challenge, Long *et al.* devised a new technique for direct *in situ* X-Ray characterisation of the adsorption of CO, CH_4, N_2, O_2, Ar, or Kr within single crystals of Co_2(dobdc) (dobdc = 2,5-dihydroxybenzenedicarboxylate). Their experimental set-up, comprising a custom-made gas cell equipped with a quartz capillary and ball valves for gas-dosing, creates an inert atmosphere with regulated gas pressure, in which no contaminants or ambient moisture can contact the mounted MOF crystal. Using this tool, they were able to elucidate Co (II) – guest interactions by SCXRD, reporting the first-ever SCXRD data on Co - CH_4 and Co - Ar interactions, as well as secondary and tertiary binding sites in Co_2(dobdc) that only become relevant at high pressures.[86]

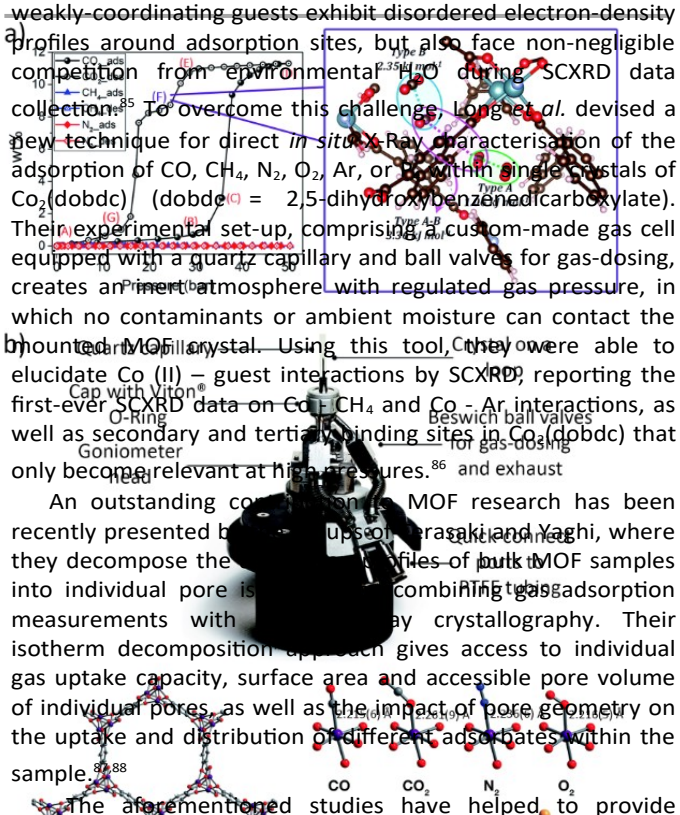

Figure 2. (a) Left: Adsorption (filled symbols) and desorption (open symbols) isotherms for **1** recorded at 298 K with test gases CO_2, CH_4, and N_2. Right: Perspective view showing CO_2 positions within the geometry-optimised structure of intermediate-state **1** with guest-guest interaction energies between different combinations of two CO molecules. (b) Top: Diagram of the gas cell used in the study reported in Reference 85. Bottom: Representation of the Co_2(dobdc) crystal structure at 298 K viewed along the c-axis (Left), and first coordination spheres for Co (II) in the structures of CO, CO_2, N_2, O_2, CH_4, Ar and P_4 at different temperatures (Right). Reproduced with permission of References 76 and 86 - Published by The Royal Society of Chemistry

An outstanding contribution to MOF research has been recently presented by Sumida, Kupsoo, Kurasaki and Yaghi, where they decompose the [illegible] files of bulk MOF samples into individual pore [illegible] combining gas adsorption measurements with [illegible]ray crystallography. Their isotherm decomposition approach gives access to individual gas uptake capacity, surface area and accessible pore volume of individual pores, as well as the impact of pore geometry on the uptake and distribution of different adsorbates within the sample.[87,88]

The aforementioned studies have helped to provide important fundamental knowledge on the chemistry and physical properties of porous materials and their interactions with gas-phase and weakly-interacting guests. This information is crucial to the design of industrial MOF-based systems for adsorption and separation processes. The examples provided highlight the importance of using SCXRD to study adsorption phenomena at the atomic level, and reflect the importance of ongoing research in this area.[89]

4. SCXRD of Covalent PSM in MOF linkers: from fundamentals to application

The interactions between MOF and guests are not limited to encapsulation processes. The latent reactivity of MOF building blocks allows for the introduction of functional groups, that may not be compatible with the MOF synthesis conditions, via PSM.[90] The combination of organic chemistry with MOFs has enabled an evolution in the synthesis of functional materials, from rudimentary "shake-and-bake" methodologies to sophisticated pore-engineering strategies.[19–21] Since the formal introduction of the field by Wang and Cohen in 2009,[18] the covalent PSM of MOFs has proven to be an efficient and flexible way to tune the surface of MOF pores, and quickly became the most widely-reported strategy due to its simplicity and well-established chemistry. To date, MOFs have been covalently modified in myriad ways, ranging from single covalent condensations[90–93] to selective orthogonal routes that generate multivariate MOF systems (MTV-MOFs).[94,95] A stunning example was reported in 2016 by Yaghi and co-workers, who performed up to seven tandem covalent PSMs within the pores of the multivariate MOF, MTV-IRMOF-74-III. The authors thus synthesised artificial enzymatic systems based on introduction of complementary amino-acid sequences periodically spaced within the MOF cavities.[96]

Nuclear Magnetic Resonance (NMR) is arguably the best routine characterisation for the structural elucidation of organic moieties and their transformations. Since most covalent PSMs have negligible effects on the framework's integrity, the evidence of functional group reactivity is clearly reflected in the NMR spectra of the product. However, the technique does not provide information of long-range distribution in routine measurements. Solid-state NMR measurements of MOF samples provide non-integrative or averaged values of PSM yields, depending on the studied nuclei, whereas digestion NMR is limited by the presence of paramagnetic metal ions in the solution and by potential fragmentation of the linkers.[97,98] While some new techniques achieve long-range order quantification by NMR techniques, these measurements require specialised equipment and large amounts of sample.[99,100]

Although the PSM of MOFs has been done for roughly two decades, to date, there are scarce reports of the study of these transformations by SCXRD.[101] This is not surprising, considering the numerous obstacles that researchers need to overcome to obtain proper diffraction data of covalently-modified MOF crystals, such as thermal motion of side groups, low conversion, and their general fragility of single-crystalline MOF samples. Additionally, most PSMs are performed on high-symmetry MOF systems, which translate to excessive disorder around the organic subunits.[85]

In 2015 Forgan and co-workers reported an example of quantitative transformations within integral components of Zr- and Hf (IV)-based MOFs via post-synthetic stereoselective bromination of internal alkyne groups (Figure 3a). Single-crystals of Zr(edb) and Hf(edb) (where edb = 4,4'-ethynyldibenzoic acid) were added to a 10 mL sample vial and solvent exchanged with $CHCl_3$ without stirring. A small amount of Br_2 was pipetted into the mixture and the vial was sealed and left to stand in the dark for 96h. The washed crystals showed a change in hybridisation of the central alkyne groups, which induced a mechanical contraction of the lattice in a single crystal-to-single crystal (SC-to-SC) fashion, with a concomitant decrease in cell volume of 3.7%.[102] The same technique was used to induce flexibility to a stilbenedicarboxylate MOF, via generation of sp^3-hybridised linker cores. However, in this case, the newly acquired flexibility in the framework precluded SCXRD data collection.[103,104] Nonetheless, both of these examples illustrate how ligand functionalisation by PSM can markedly affect the mechanical properties of MOFs, and how such modifications can yield otherwise inaccessible materials that exhibit high conformational freedom.

A more recent example of covalent PSM with subsequent characterisation by SCXRD was described by Maspoch and co-workers, who reported the first example of SC-to-SC transformation within a UiO-66-type MOF via solid/gas phase reactivity.[105] In a typical experiment, a solid mixture of bulk and single-crystal ZrEBDC (where EBDC = 2-ethenylbenzene-1,4-dicarboxylic acid) was packed inside a U-shaped Pyrex tube and immersed in an acetone:CO_2 bath at -78 ºC. By flowing a constant ozone stream through the tube, the authors achieved quantitative transformation of the pendant olefin chain substituents into 1,2,4-trioxolane rings in less than 30 minutes (Figure 3b). Here, the main limitation of covalent PSMs (*vide supra*) was obviated, as the gas-phase diffusion of O_3 proceeds without kinetic restraint. In this study, SCXRD was the most

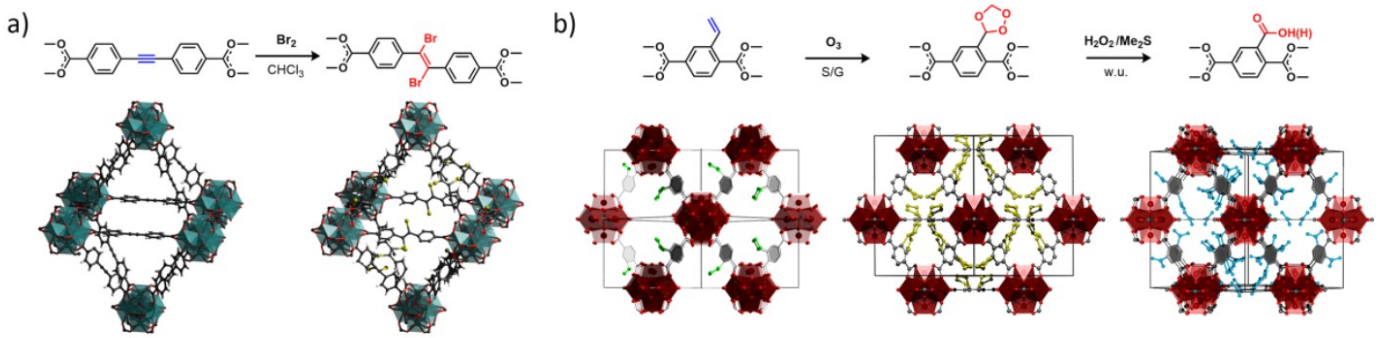

Figure 3. (a) Schematic of crystalline structures of the post-synthetic bromination of a Zr(IV)-based MOF, transforming the central alkyne groups in the ligand to the bromination product. (b) Schematic of the crystalline structures of a two-step post-synthetic ozonolysis of an olefin-tagged Zr(IV)-based MOF. First step: solid-gas phase ozonolysis to obtain 1,2,4-trioxolane intermediates. Second step: oxidative(H_2O_2) or reductive (Me_2S) work-up processes to obtain CHO- and COOH-functionalised MOFs, respectively. Reprinted (adapted) with permission from References 102 and 105 - Copyright 2015/2018 American Chemical Society.

precise technique to verify the formation of metastable trioxolanes within the porous matrix. NMR studies required the digestion of the samples under acid media, which fragmented the trioxolanes into a mixture of solvated species (specifically, metathesis cross-ozonation and oxidative cleavage by-products), precluding a direct study of the reaction evolution. In contrast with the volatile nature of molecular trioxolanes,[106,107] the MOF-confined counterparts were synergistically stabilised within the backbone, even under standard activation conditions. Further work-up in liquid phase (diluted DMF solutions of Me_2S or H_2O_2, respectively) enabled a second SC-to-SC transformation into either aldehydes or carboxylic acids, the latter in quantitative yield. As a mild selective chemistry, properly understood by SCXRD, solid-gas phase ozonolysis has been implemented in applied MOF research for generating hierarchical porosity in engineered MOF systems.[108,109] These studies further demonstrate how SCXRD can provide invaluable structural insight on pore-engineering, and how an in-depth understanding of MOFs chemistry can advance elegant chemistry from proof-of-concept to practical applications.

The covalent PSM of MOFs is not limited to the insertion of external moieties. When exposed to external stimuli (*e.g.* temperature, light, pressure), some *a-priori* robust MOFs, with chemically-stable linkers, can reveal latent reactivity. In these cases, the diffusion of reagents is irrelevant, which in turn enables higher and faster conversion rates. Here, the relative orientation and preorganisation of the linkers is critical to proceed correctly. An interesting example was reported in 2019 by Vittal *et al.*, who explored the [2+2] cycloaddition reaction between the pillaring 4,4'-bipyridylethylene (bpe) linkers of a Cd (II)-based MOF. In this MOF, the olefin bond pairs in adjacent bpe ligands are aligned in parallel, thus satisfying Schmidt's criteria for a [2+2] cycloaddition reaction. Although cycloaddition reactions had already been reported in MOFs, the work by Vittal and co-workers provided significant insight into the use of photochemistry to create different chemical patterns within a lattice. Their study, based on SC-to-SC chemistry, elucidated that opposite reaction outcomes are dictated by subtle modifications in the solvated state of the MOF and crystal orientation. Thus, they were able to introduce heterogeneous patterns in the MOF, without any concomitant loss of characteristic long-range order.[110]

The reactivity of MOF linkers is expansive. From the simplest condensations to multistep orthogonal pathways, covalent transformations represent a powerful method for finely tuning the physical properties of MOFs. However, functionalisation proceeds through heterogeneous processes, which lead to increasing levels of complexity and might favour unexpected reactions.[111] Accordingly, limiting the study of these steps to readily available techniques might lead to inaccurate characterisation of the true composition within the functionalised material. In this context, SCXRD has proven to be an efficient technique for structural characterisation of these molecular-level transformations, with an eye to potential applications. Through covalent deprotection, the groups of Telfer and Richardson exploited the use of PSM chemistry to generate active moieties *in situ* within MOF pores.[112–116] These examples clearly show that such chemistry can advance fields such as catalysis where precise control of active sites is desired.

5. Crystallographic insights of catalytically-active species within MOF pores

Industrial chemicals are typically produced via large-scale synthesis faciltiated by inorganic and organometallic catalysts. Understanding the mechanism of how these reactions proceed is essential for the design of new or improved catalysts with better activity, selectivity, and overall efficiency. Whilst laser-pulsed techniques can track the dynamic evolution of solvated catalysts in situ,[117,118] SCXRD provides atomic-scale information and absolute configuration of these highly-reactive species.[119,120] Diffraction data can be obtained either by low-temperature isolation of intermediate species[121,122] or by their occlusion within crystalline matrices.[123] MOFs are attractive candidates for the latter thanks to their tuneable structure, which enables the insertion and site-isolation of catalytically-active species into their porous cavities,[124,125] inorganic nodes,[126–130] and organic backbone.[131–134] In the last decade, MOFs have been widely used as solid supports for the accommodation and periodic spacing of catalytic species, ranging from metal and metal-oxide nanoparticles[135–138] to isolated coordination complexes,[139–141] with remarkable effects on their long-term stability and reactivity. Additionally, the crystalline nature of MOFs permits the examination of the catalyst structure post reaction via SCXRD. An illustrative example is the work of Pardo and co-workers, who synthesised naked $[Pd_4]^{0/1+}$ clusters within the cavities of an anionic bimetallic MOF ($Ni_2\{Ni_4[Cu_2(L)_2]_3\}$) via a three-step synthesis involving quantitative transmetalation, stoichiometric ion exchange, and in situ reduction (Figure 4a).[142] The robustness and high crystallinity of the MOF played an important role in the process. Immersing the parent MOF crystals in a diluted aqueous solution of $Pd(NH_3)_4Cl_2$, followed by further reduction with 26 successive aliquots of $NaBH_4$ generated Pd_4 units encapsulated within the ~2 nm hydrophilic octagonal pockets of lattice. This work was the first report of a linear Pd_4 cluster, and thus SCXRD proved to be unvaluable in the detection of this new species. A similar approach was applied in different MOF families to obtain the crystalline structure of important reactive species ($[Pt_2]^0$, Pt^{1+}, Au^{1+}/Au^{3+}, Ru^{3+}).[143–147] Remarkably, the resulting catalysts showed outstanding efficiency, outperforming state-of-the-art competitors in yields and turnover numbers.

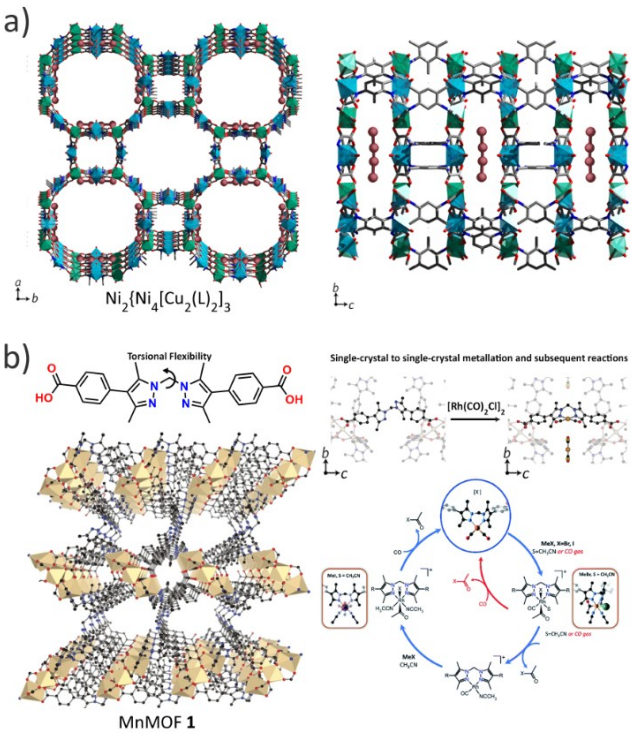

Figure 4. (a) Perspective view of Pd_4-loaded $Ni_2\{Ni_4[Cu_2(L)_2]_3$ (left) and an enlargement of the single channel along the *a* axis (right). (b) Crystalline structure of MnMOF **1** and subsequent post-synthetic metalation and transformations of the newly-inserted metallic centres. Reproduced with permission of References 142, 148 and 152 – Copyright 2014/2017 Nature Publishing Group. Copyright 2017 Wiley-VCH.

Apart from trapping reactive species within MOF pores/pockets, the hybrid nature of MOFs permits the incorporation of covalently anchored species within the organic backbone. Through this strategy, MOFs have been tailored with site-isolated coordination/organometallic complexes. However, such systems proved challenging to characterise by SCXRD, since the lower electron-density and free rotation around MOF linkers generates disordered electron density around the guest, particularly in MOFs with high-symmetry systems. In 2014, the Sumby-Doonan group reported a flexible Mn(II)-based MOF **1** (1 = $[Mn_3L_2L']$; where L and L' are crystallographically-independent forms of the ligand bis(4-(4-carboxyphenyl)-1H-3,5-dimethylpyrazolyl)methane, Figure 4b) with strong chelating properties that derive from periodically-lined, vacant, bis-pyrazolate moieties within its porous channels. **1** crystallises in a monoclinic, low-symmetry group ($P2_1/c$), in which each pore presents a full-occupancy, framework-bound, L'-coordination site, poised for post-synthetic metalation.[148] The inherent flexibility of MnMOF **1** has enabled the quantitative insertion of several metallic species (***e.g.*** Cu (II), Co (II), Zn (II), Mn (II), Rh (I)) via post-synthetic metalation in quantitative yields, with no significant loss in crystallinity.[148–150] MnMOF **1** proved to be an excellent platform for the structural elucidation of anchored catalytic species via SCXRD: in such a low-symmetry environment, both the primary and secondary coordination spheres around the metal can be precisely elucidated — not only on its initial state, but also after subsequent post-synthetic transformations (*i.e.* ion exchange, oxidative addition, migratory insertion).[151,152] Indeed, covalently anchoring reactive species within the low-symmetry bis-pyrazolate groups heavily reduces the degrees of freedom of inserted species, thus reducing structural disorder during SCXRD data collection. In their most recent example, the group exploited the inherent crystallinity of MnMOF **1** to explore ethylene hydrogenation and butene isomerisation cycles of anchored Rh (I) species.[153] Their study, supported by SCXRD and gas-phase NMR, demonstrated the strong influence of the present counter-anion (second sphere) during the solid-gas phase[154] catalytic cycle. The presence of coordinating anions (Cl^-) gave negligible catalytic activity, inhibited by strong interactions between allyl/propyl hydride intermediates and Cl^-. In contrast, the BF_4^- species did not exhibit any interaction with the metal core, thus rapidly catalysing the reaction with a TOF of 2000 h^{-1} over five cycles. Single-crystal manipulation proved to be critical in this project in order to isolate the reactive $Rh^I(C_2H_4)_2^+$ and $Rh^I(NBD)^+$ species and subsequent

intermediates within the MOF pores. Both the metalation of MnMOF **1** and ion exchange steps were done in a SC-to-SC fashion under a dry ethylene atmosphere (> 1 bar) in glass pressure vessels fitted with a pressure gauge and Swagelok tap assembly. These conditions favoured the insertion of single-atom Rh(I) species within the bis-pyrazolate centers of MnMOF **1** and avoided the formation of Rh (0) nanoparticles.

These examples illustrate the value of SCXRD to gain detailed structural insights on MOFs, their site isolation capabilities and guest chemistry.[155] This technique has already underpinned significant advances in homogeneous systems, and by tailoring active species within crystalline MOFs, SCXRD can finally compensate the lack of catalyst design in heterogeneous catalysis.

6. Summary and outlook

With thousands of MOF papers entering the literature each year, one could envisage that MOFs may slowly displace zeolites, silicas or active carbons from sectors where they are still the material of choice. Indeed, in recent years MOFs have made significant inroads in niche applications, for example atmospheric water harvesting.[99,156,157] In reality though, the production costs and poor recyclability are considered road-blocks to their commercialisation.[158] At present, MOFs have to compete with qualities that cheaper alternatives lack to make their manufacturing viable, such as the ability to engineer pore size and functionality with molecular precision. Thus, structure determination is arguably the most important characterization technique for MOFs. Fortunately, most MOF research groups have direct and routine accessibility to SCXRD data collection, either via in-house single-crystal diffractometers or through synchrotron facilities. However, SCXRD should not be seen as a technique that exclusively provides conclusive and irrefutable data. The quality, and thus interpretation, of the collected data is affected by both by the size and stability of the mounted crystal. Given that a general method to grow MOF crystals suitable for SCXRD does not exist,[159,160] many MOF structures cannot be elucidated by SCXRD. However, recently, Three-Dimensional Electron Diffraction (3DED) methods have been applied to determine the structures of several microcrystalline samples which are incompatible with the requirements for SCXRD.[161] Crystals that are several orders of magnitude smaller than those required for X-ray analysis can be used for high-resolution structural elucidation, which omits the arduous, and potentially fruitless, step of growing micrometre-sized MOF crystals. Recent reviews published by Zou *et. al.* describe the development, advances and limitations of this young field for collecting MOF structural data.[162,163]

While significant advances in understanding the PSM chemistry of single-crystal MOFs have been made, most of these studies have been carried out on rigid, high-symmetry lattices that limit the scope of the approach. The judicious design, synthesis and crystallisation of low-symmetry MOF platforms with inherent flexibility, torsional movement and full occupancy around the newly-generated functionalities will facilitate further progress. Furthermore, given the recent developments in the areas of Reticular Chemistry,[164] geometry mismatch,[165] and orthogonal post-synthetic reactivity,[166] it can be anticipated that structural characterisation will remain of significant importance. It can be argued that the catalysis field has benefited the most from the recent advances in MOF chemistry. MOFs offer unparalleled versatility for the encapsulation, site-isolation, and stabilisation of highly-active organic and organometallic catalysts. As we have highlighted MOF architectures have already been employed as crystalline matrices for the visualisation of highly reactive and novel catalytic species (Section 5) via SCXRD and we believe this area of research will continue to provide valuable information for catalytic processes.

The examples we have canvassed are not exhaustive but point towards how the development of new areas in MOF chemistry will be underpinned by SCXRD. Given that MOFs show a remarkable structure-function relationship, atomic-level information will remain crucial to understanding fundamental aspects of MOF chemistry and developing future applications. Lastly, we would like to note that although this highlight is MOF-centred, the principles we have covered apply to other crystalline porous materials such as Covalent Organic Frameworks (COFs), Metal-Organic Polyhedra (MOPs), Porous Organic Cages (POCs), or Hydrogen-Bonded Organic Frameworks (HOFs). Despite the fact that their chemistry is not as developed in terms of guest interactions, post-synthetic modifications or industrial-scale application, all of these materials possess similar potential to MOFs, and may be a preferable platform for some applications.

Conflicts of interest

The authors declare that there are no conflicts of interest.

Acknowledgements

This work was supported by the Spanish MINECO (project RTI2018-095622-B-I00) and the Catalan AGAUR (project 2017 SGR 238). It was also funded by the CERCA Program/Generalitat de Catalunya. ICN2 is supported by the Severo Ochoa program from the Spanish MINECO (Grant No. SEV-2017-0706). CJS and CJD gratefully acknowledge the Australian Research Council for funding (DP190101402).

References

1 H. Furukawa, K. E. Cordova, M. O'Keeffe and O. M. Yaghi, *Science*, 2013, **341**, 1230444.

2 U. Mueller, M. Schubert, F. Teich, H. Puetter, K. Schierle-Arndt and J. Pastré, *J. Mat. Chem.*, 2006, **16**, 626-636.

3 A. U. Czaja, N. Trukhan and U. Müller, *Chem. Soc. Rev.*, 2009, **38**, 1284-1293.

4 R. Ricco, C. Pfeiffer, K. Sumida, C. J. Sumby, P. Falcaro, S. Furukawa, N. R. Champness and C. J. Doonan, *CrystEngComm*, 2016, **18**, 6532-6542.

5 M. J. Kalmutzki, N. Hanikel and O. M. Yaghi, *Sci. Adv.*, 2018, **4**, eaat9180.

6 H. Furukawa, N. Ko, Y. B. Go, N. Aratani, S. B. Choi, E. Choi, A. Ö. Yazaydin, R. Q. Snurr, M. O'Keeffe, J. Kim and O. M. Yaghi, *Science*, 2010, **329**, 424-428.

7 X. Han, S. Yang and M. Schröder, *Nat. Rev. Chem.*, 2019, **3**, 108-118.

8 A. Bavykina, N. Kolobov, I. S. Khan, J. A. Bau, A. Ramirez and J. Gascon, *Chem. Rev.*, 2020, **120**, 8468–8535.

9 R. B. Lin, S. Xiang, W. Zhou and B. Chen, *Chem*, 2020, 6, 337–363.

10 W. Cui, T. Hu and X. Bu, *Adv. Mater.*, 2020, **32**, 1806445.

11 Z. Zhang, Z. Z. Yao, S. Xiang and B. Chen, *Energy Environ. Sci.*, 2014, **7**, 2868–2899.

12 A. J. Rieth and M. Dinca, *J. Am. Chem. Soc.*, 2018, **140**, 3461–3466.

13 J. Li, P. M. Bhatt, J. Li, M. Eddaoudi and Y. Liu, *Adv. Mater.*, 2020, **32**, 2002563.

14 S. Rojas, I. Colinet, D. Cunha, T. Hidalgo, F. Salles, C. Serre, N. Guillou and P. Horcajada, *ACS Omega*, 2018, **3**, 2994–3003.

15 S. Rojas, A. Arenas-Vivo and P. Horcajada, *Coord. Chem. Rev.*, 2019, **388**, 202–226.

16 H. Amer Hamzah, W. J. Gee, P. R. Raithby, S. J. Teat, M. F. Mahon and A. D. Burrows, *Chem. - A Eur. J.*, 2018, **24**, 11094–11102.

17 W. T. Kou, C. X. Yang and X. P. Yan, *J. Mater. Chem. A*, 2018, **6**, 17861–17866.

18 Z. Wang and S. M. Cohen, *Chem. Soc. Rev.*, 2009, **38**, 1315–1329.

19 K. K. Tanabe and S. M. Cohen, *Chem. Soc. Rev.*, 2011, **40**, 498–519.

20 S. M. Cohen, *Chem. Rev.*, 2012, **112**, 970–1000.

21 S. M. Cohen, *J. Am. Chem. Soc.*, 2017, **139**, 2855–2863.

22 M. Kalaj and S. M. Cohen, *ACS Cent. Sci.*, 2020, **6**, 1046–1057.

23 L. Xu, Y. Luo, L. Sun, S. Pu, M. Fang, R. X. Yuan and H. Bin Du, *Dalt. Trans.*, 2016, **45**, 8614–8621.

24 E. Brunner and M. Rauche, *Chem. Sci.*, 2020, **11**, 4297–4304.

25 C. Liu, C. Zeng, T. Y. Luo, A. D. Merg, R. Jin and N. L. Rosi, *J. Am. Chem. Soc.*, 2016, **138**, 12045–12048.

26 J. P. Zhang, P. Q. Liao, H. L. Zhou, R. B. Lin and X. M. Chen, *Chem. Soc. Rev.*, 2014, **43**, 5789–5814.

27 M. Mon, R. Bruno, J. Ferrando-Soria, L. Bartella, L. Di Donna, M. Talia, R. Lappano, M. Maggiolini, D. Armentano and E. Pardo, *Mater. Horizons*, 2018, **5**, 683–690.

28 C. A. Trickett, K. J. Gagnon, S. Lee, F. Gándara, H. B. Bürgi and O. M. Yaghi, *Angew. Chem., Int. Ed.*, 2015, **54**, 11162–11167.

29 Y. Inokuma, T. Arai and M. Fujita, *Nat. Chem.*, 2010, **2**, 780–783.

30 M. Yoshizawa, J. K. Klosterman and M. Fujita, *Angew. Chem., Int. Ed.*, 2009, **48**, 3418–3438.

31 T. Kawamichi, T. Kodama, M. Kawano and M. Fujita, *Angew. Chem., Int. Ed.*, 2008, **47**, 8030–8032.

32 Y. Inokuma, M. Kawano and M. Fujita, *Nat. Chem.*, 2011, **3**, 349–358.

33 A. Nuñez-Lopez, M. Galbiati, N. M. Padial, C. R. Ganivet, S. Tatay, E. Pardo, D. Armentano and C. Martí-Gastaldo, *Angew. Chem., Int. Ed.*, 2019, **58**, 9179–9183.

34 M. Hoshino, A. Khutia, H. Xing, Y. Inokuma and M. Fujita, *IUCrJ*, 2016, **3**, 139–151.

35 N. Wada, R. D. Kersten, T. Iwai, S. Lee, F. Sakurai, T. Kikuchi, D. Fujita, M. Fujita and J.-K. Weng, *Angew. Chem., Int. Ed.*, 2018, **57**, 3671–3675.

36 T. Mitsuhashi, T. Kikuchi, S. Hoshino, M. Ozeki, T. Awakawa, S. P. Shi, M. Fujita and I. Abe, *Org. Lett.*, 2018, **20**, 5606–5609.

37 W. De Poel, P. T. Tinnemans, A. L. L. Duchateau, M. Honing, F. P. J. T. Rutjes, E. Vlieg and R. De Gelder, *Cryst. Growth Des.*, 2018, **18**, 126–132.

38 S. Urban, R. Brkljača, M. Hoshino, S. Lee and M. Fujita, *Angew. Chem., Int. Ed.*, 2016, **55**, 2678–2682.

39 R. D. Kersten, S. Lee, D. Fujita, T. Pluskal, S. Kram, J. E. Smith, T. Iwai, J. P. Noel, M. Fujita and J. K. Weng, *J. Am. Chem. Soc.*, 2017, **139**, 16838–16844.

40 N. Zigon, T. Kikuchi, J. Ariyoshi, Y. Inokuma and M. Fujita, *Chem. - An Asian J.*, 2017, **12**, 1057–1061.

41 S. Yoshioka, Y. Inokuma, V. Duplan, R. Dubey and M. Fujita, *J. Am. Chem. Soc.*, 2016, **138**, 10140–10142.

42 S. Sairenji, T. Kikuchi, M. A. Abozeid, S. Takizawa, H. Sasai, Y. Ando, K. Ohmatsu, T. Ooi and M. Fujita, *Chem. Sci.*, 2017, **8**, 5132–5136.

43 K. Yan, R. Dubey, T. Arai, Y. Inokuma and M. Fujita, *J. Am. Chem. Soc.*, 2017, **139**, 11341–11344.

44 V. Duplan, M. Hoshino, W. Li, T. Honda and M. Fujita, *Angew. Chem., Int. Ed.*, 2016, **55**, 4919–4923.

45 G. H. Ning, K. Matsumura, Y. Inokuma and M. Fujita, *Chem. Commun.*, 2016, **52**, 7013–7015.

46 Y. Inokuma, S. Yoshioka, J. Ariyoshi, T. Arai, Y. Hitora, K. Takada, S. Matsunaga, K. Rissanen and M. Fujita, *Nature*, 2013, **495**, 461–466.

47 T. R. Ramadhar, S. L. Zheng, Y. S. Chen and J. Clardy, *Acta Crystallogr. Sect. A Found. Crystallogr.*, 2015, **71**, 46–58.

48 W. Poel, P. Tinnemans, A. L. L. Duchateau, M. Honing, F. P. J. T. Rutjes, E. Vlieg and R. Gelder, *Chem. – A Eur. J.*, 2019, **25**, 14999–15003.

49 Q. Du, J. Peng, P. Wu and H. He, *TrAC - Trends Anal. Chem.*, 2018, **102**, 290–310.

50 S. Lee, E. A. Kapustin and O. M. Yaghi, *Science,* 2016, **353**, 808-811.

51 L. Rosenberger, C. Von Essen, A. Khutia, C. Kühn, K. Urbahns, K. Georgi, R. W. Hartmann and L. Badolo, *Drug Metab. Dispos.*, 2020, **48**, 587–593.

52 M. Agrawal and D. S. Sholl, *ACS Appl. Mater. Interfaces*, 2019, **11**, 31060–31068.

53 P. Zhao, H. Fang, S. Mukhopadhyay, A. Li, S. Rudić, I. J. McPherson, C. C. Tang, D. Fairen-Jimenez, S. C. E. Tsang and S. A. T. Redfern, *Nat. Commun.*, 2019, **10**, 1–8.

54 J. L. C. Rowsell, E. C. Spencer, J. Eckert, J. A. K. Howard and O. M. Yaghi, *Science*, 2005, **309**, 1350–1354.

55 E. J. Carrington, I. J. Vitórica-Yrezábal and L. Brammer, *Acta Crystallogr. Sect. B Struct. Sci. Cryst. Eng. Mater.*, 2014, **70**, 404–422.

56 P. Lama and L. J. Barbour, *J. Am. Chem. Soc.*, 2018, **140**, 2145–2150.

57 S. Nandi, R. Maity, D. Chakraborty, H. Ballav and R. Vaidhyanathan, *Inorg. Chem.*, 2018, **57**, 5267–5272.

58 C. Yang, X. Wang and M. A. Omary, *Angew. Chem., Int. Ed.*, 2009, **48**, 2500–2505.

59 A. Schneemann, V. Bon, I. Schwedler, I. Senkovska, S. Kaskel and R. A. Fischer, *Chem. Soc. Rev.*, 2014, **43**, 6062–6096.

60 T. Kundu, M. Wahiduzzaman, B. B. Shah, G. Maurin and D. Zhao, *Angew. Chem., Int. Ed.*, 2019, **58**, 8073–8077.

61 M. Alhamami, H. Doan and C.-H. Cheng, *Materials*, 2014, **7**, 3198–3250.

62 A. Sławek, J. M. Vicent-Luna, B. Marszałek, B. Gil, R. E. Morris, W. Makowski and S. Calero, *Chem. Mater.*, 2018, **30**, 5116–5127.

63 T. W. Tseng, L. W. Lee, T. T. Luo, P. H. Chien, Y. H. Liu, S. L. Lee, C. M. Wang and K. L. Lu, *Dalt. Trans.*, 2017, **46**, 14728–14732.

64 F. Formalik, A. V. Neimark, J. Rogacka, L. Firlej and B. Kuchta, *J. Colloid Interface Sci.*, 2020, **578**, 77–88.

65 H. J. Choi, M. Dinca and J. R. Long, *J. Am. Chem. Soc*, 2008, **130**, 7848–7850.

66 S. Rahman, A. Arami-Niya, X. Yang, G. Xiao, G. (Kevin) Li and E. F. May, *Commun. Chem.*, 2020, **3**, 1–6.

67 S. A. Sapchenko, M. O. Barsukova, R. V. Belosludov, K. A. Kovalenko, D. G. Samsonenko, A. S. Poryvaev, A. M. Sheveleva, M. V. Fedin, A. S. Bogomyakov, D. N. Dybtsev, M. Schröder and V. P. Fedin, *Inorg. Chem.*, 2019, **58**, 6811–6820.

68 S. Krause, V. Bon, I. Senkovska, U. Stoeck, D. Wallacher, D. M. Többens, S. Zander, R. S. Pillai, G. Maurin, F. X. Coudert and S. Kaskel, *Nature*, 2016, **532**, 348–352.

69 J. D. Evans, L. Bocquet and F. X. Coudert, *Chem*, 2016, **1**, 873–886.

70 S. Krause, J. D. Evans, V. Bon, I. Senkovska, S. Ehrling, U. Stoeck, P. G. Yot, P. Iacomi, P. Llewellyn, G. Maurin, F. X. Coudert and S. Kaskel, *J. Phys. Chem. C*, 2018, **122**, 19171–19179.

71 S. Krause, J. D. Evans, V. Bon, I. Senkovska, F.-X. Coudert, D. M. Többens, D. Wallacher, N. Grimm and S. Kaskel, *Faraday Discuss.*,2021, *Advance Article* (DOI:10.1039/d0fd00013b).

72 S. M. J. Rogge, R. Goeminne, R. Demuynck, J. J. Gutiérrez-Sevillano, S. Vandenbrande, L. Vanduyfhuys, M. Waroquier, T. Verstraelen and V. Van Speybroeck, *Adv. Theory Simulations*, 2019, **2**, 1800177.

73 L. Chen, J. P. S. Mowat, D. Fairen-Jimenez, C. A. Morrison, S. P. Thompson, P. A. Wright and T. Düren, *J. Am. Chem. Soc.*, 2013, **135**, 15763–15773.

74 J. Schaber, S. Krause, S. Paasch, I. Senkovska, V. Bon, D. M. Többens, D. Wallacher, S. Kaskel and E. Brunner, *J. Phys. Chem. C*, 2017, **121**, 5195–5200.

75 B. Garai, V. Bon, S. Krause, F. Schwotzer, M. Gerlach, I. Senkovska and S. Kaskel, *Chem. Mater.*, 2020, **32**, 889–896.

76 A. Hazra, D. P. Van Heerden, S. Sanyal, P. Lama, C. Esterhuysen and L. J. Barbour, *Chem. Sci.*, 2019, **10**, 10018–10024.

77 B. Pato-Doldán, M. H. Rosnes, D. Chernyshov and P. D. C. Dietzel, *CrystEngComm*, 2020, **22**, 4353–4358.

78 R. G. Miller, M. R. Warren, D. R. Allan and S. Brooker, *Inorg. Chem.*, 2020, **59**, 6376–6381.

79 A. J. Campanella, B. A. Trump, E. J. Gosselin, E. D. Bloch and C. M. Brown, *Chem. Commun.*, 2020, **56**, 2574–2577.

80 X. Liu, X. Wang and F. Kapteijn, *Chem. Rev.*, 2020, **120**, 8303–8377

81 N. C. Burtch, I. M. Walton, J. T. Hungerford, C. R. Morelock, Y. Jiao, J. Heinen, Y. S. Chen, A. A. Yakovenko, W. Xu, D. Dubbeldam and K. S. Walton, *Nat. Chem.*, 2020, **12**, 186–192.

82 J. H. Song, D. W. Kim, D. W. Kang, W. R. Lee and C. S. Hong, *Chem. Commun.*, 2019, **55**, 9713–9716.

83 M. H. Rosnes, D. Sheptyakov, A. Franz, M. Frontzek, P. D. C. Dietzel and P. A. Georgiev, *Phys. Chem. Chem. Phys.*, 2017, **19**, 26346–26357.

84 J. Sundberg, L. J. Cameron, P. D. Southon, C. J. Kepert and C. J. McKenzie, *Chem. Sci.*, 2014, **5**, 4017–4025.

85 S. Øien-ØDegaard, G. C. Shearer, D. S. Wragg and K. P. Lillerud, *Chem. Soc. Rev.*, 2017, **46**, 4867–4876.

86 M. I. Gonzalez, J. A. Mason, E. D. Bloch, S. J. Teat, K. J. Gagnon, G. Y. Morrison, W. L. Queen and J. R. Long, *Chem. Sci.*, 2017, **8**, 4387–4398.

87 H. Sung Cho, H. Deng, K. Miyasaka, Z. Dong, M. Cho, A. V. Neimark, J. Ku Kang, O. M. Yaghi and O. Terasaki, *Nature*, 2015, **527**, 503–507.

88 H. S. Cho, J. Yang, X. Gong, Y. B. Zhang, K. Momma, B. M. Weckhuysen, H. Deng, J. K. Kang, O. M. Yaghi and O. Terasaki, *Nat. Chem.*, 2019, **11**, 562–570.

89 V. Bon, E. Brunner, A. Pöppl and S. Kaskel, *Adv. Funct. Mater.*, 2020, **30**, 1907847.

90 W. J. Gee, L. K. Cadman, H. Amer Hamzah, M. F. Mahon, P. R. Raithby and A. D. Burrows, *Inorg. Chem.*, 2016, **55**, 10839–10842.

91 S. J. Garibay and S. M. Cohen, *Chem. Commun.*, 2010, **46**, 7700–7702.

92 S. Rager, M. Dogru, V. Werner, A. Gavryushin, M. Götz, H. Engelke, D. D. Medina, P. Knochel and T. Bein, *CrystEngComm*, 2017, **19**, 4886–4891.

93 E. Dugan, Z. Wang, M. Okamura, A. Medina and S. M. Cohen, *Chem. Commun.*, 2008, **29**, 3366–3368.

94 S. Wang, Y. Chen, S. Wang, P. Li, C. A. Mirkin and O. K. Farha, *J. Am. Chem. Soc.*, 2019, **141**, 2215–2219.

95 M. Kim, J. F. Cahill, K. A. Prather and S. M. Cohen, *Chem. Commun.*, 2011, **47**, 7629–7631.

96 A. M. Fracaroli, P. Siman, D. A. Nagib, M. Suzuki, H. Furukawa, F. D. Toste and O. M. Yaghi, *J. Am. Chem. Soc.*, 2016, **138**, 8352–8355.

97 L. Garzón-Tovar, S. Rodríguez-Hermida, I. Imaz and D. Maspoch, *J. Am. Chem. Soc.*, 2017, **139**, 897–903.

98 H. Amer Hamzah, T. S. Crickmore, D. Rixson and A. D. Burrows, *Dalt. Trans.*, 2018, **47**, 14491–14496.

99 X. Kong, H. Deng, F. Yan, J. Kim, J. A. Swisher, B. Smit, O. M. Yaghi and J. A. Reimer, *Science (80-.).*, 2013, **341**, 882–885.

100 J. Tang, S. Li, Y. Su, Y. Chu, J. Xu and F. Deng, *J. Phys. Chem. C*, 2020, **124**, 17640–17647.

101 K. K. Tanabe, C. A. Allen and S. M. Cohen, *Angew. Chem., Int. Ed.*, 2010, **49**, 9730–9733.

102 R. J. Marshall, S. L. Griffin, C. Wilson and R. S. Forgan, *J. Am. Chem. Soc.*, 2015, **137**, 9527–9530.

103 R. J. Marshall, S. L. Griffin, C. Wilson and R. S. Forgan, *Chem. - A Eur. J.*, 2016, **22**, 4870–4877.

104 R. J. Marshall, T. Richards, C. L. Hobday, C. F. Murphie, C. Wilson, S. A. Moggach, T. D. Bennett and R. S. Forgan, *Dalt. Trans.*, 2016, **45**, 4132–4135.

105 J. Albalad, H. Xu, F. Gándara, M. Haouas, C. Martineau-Corcos, R. Mas-Ballesté, S. A. Barnett, J. Juanhuix, I. Imaz and D. Maspoch, *J. Am. Chem. Soc.*, 2018, **140**, 2028–2031.

106 R. Willand-Charnley, T. J. Fisher, B. M. Johnson and P. H. Dussault, *Org. Lett.*, 2012, **14**, 2242–2245.

107 C. E. Schiaffo and P. H. Dussault, *J. Org. Chem.*, 2008, **73**, 4688–4690.

108 Y. Song, X. Feng, J. S. Chen, C. Brzezinski, Z. Xu and W. Lin, *J. Am. Chem. Soc.*, 2020, **142**, 4872–4882.

109 V. Guillerm, H. Xu, J. Albalad, I. Imaz and D. Maspoch, *J. Am. Chem. Soc.*, 2018, **140**, 15022–15030.

110 I. Park, E. Lee, S. S. Lee and J. J. Vittal, *Angew. Chem., Int. Ed.*, 2019, **58**, 14860–14864.

111 M. Kalaj and S. M. Cohen, *ACS Cent. Sci.*, 2020, **6**, 1046–1057.

112 A. Alkaş, L. E. S. Friche, S. N. Harris and S. G. Telfer, *Chem. – A Eur. J.*, 2020, **26**, 10321–10329.

113 R. K. Deshpande, J. L. Minnaar and S. G. Telfer, *Angew. Chem., Int. Ed.*, 2010, **49**, 4598–4602.

114 M. R. Bryant, T. A. Ablott, S. G. Telfer, L. Liu and C. Richardson, *CrystEngComm*, 2019, **21**, 60–64.

115 M. R. Bryant and C. Richardson, *CrystEngComm*, 2015, **17**, 8858–8863.

116 A. D. Burrows, S. O. Hunter, M. F. Mahon and C. Richardson, *Chem. Commun.*, 2013, **49**, 990–992.

117 M. K. Kuimova, W. Z. Alsindi, J. Dyer, D. C. Grills, O. S. Jina, P. Matousek, A. W. Parker, P. Portius, X. Zhong Sun, M. Towrie, C. Wilson, J. Yang and M. W. George, *J. Chem. Soc. Dalt. Trans.*, 2003, **3**, 3996–4006.

118 S. A. Bartlett, N. A. Besley, A. J. Dent, S. Diaz-Moreno, J. Evans, M. L. Hamilton, M. W. D. Hanson-Heine, R. Horvath, V. Manici, X. Z. Sun, M. Towrie, L. Wu, X. Zhang and M. W. George, *J. Am. Chem. Soc.*, 2019, **141**, 11471–11480.

119 H. D. Flack and G. Bernardinelli, *Chirality*, 2008, **20**, 681–690.

120 F. M. Chadwick, A. I. McKay, A. J. Martinez-Martinez, N. H. Rees, T. Krämer, S. A. Macgregor and A. S. Weller, *Chem. Sci.*, 2017, **8**, 6014–6029.

121 L. Jin, D. R. Tolentino, M. Melaimi and G. Bertrand, *Sci. Adv.*, 2015, **1**, e1500304.

122 V. Vasilenko, C. K. Blasius, H. Wadepohl and L. H. Gade, *Chem. Commun.*, 2020, **56**, 1203–1206.

123 W. M. Bloch, N. R. Champness and C. J. Doonan, *Angew. Chem., Int. Ed.*, 2015, **54**, 12860–12867.

124 M. Kawano and M. Fujita, *Coord. Chem. Rev.*, 2007, **251**, 2592–2605.

125 O. Ohmori, M. Kawano and M. Fujita, *J. Am. Chem. Soc.*, 2004, **126**, 16292–16293.

126 K. I. Otake, Y. Cui, C. T. Buru, Z. Li, J. T. Hupp and O. K. Farha, *J. Am. Chem. Soc.*, 2018, **140**, 8652–8656.

127 Z. Li, A. W. Peters, V. Bernales, M. A. Ortuño, N. M. Schweitzer, M. R. Destefano, L. C. Gallington, A. E. Platero-Prats, K. W. Chapman, C. J. Cramer, L. Gagliardi, J. T. Hupp and O. K. Farha, *ACS Cent. Sci.*, 2017, **3**, 31–38.

128 V. Bernales, D. Yang, J. Yu, G. Gümüşlu, C. J. Cramer, B. C. Gates and L. Gagliardi, *ACS Appl. Mater. Interfaces*, 2017, **9**, 33511–33520.

129 D. Yang, S. O. Odoh, J. Borycz, T. C. Wang, O. K. Farha, J. T. Hupp, C. J. Cramer, L. Gagliardi and B. C. Gates, *ACS Catal.*, 2016, **6**, 235–247.

130 N. Van Velthoven, S. Waitschat, S. M. Chavan, P. Liu, S. Smolders, J. Vercammen, B. Bueken, S. Bals, K. P. Lillerud, N. Stock and D. E. De Vos, *Chem. Sci.*, 2019, **10**, 3616–3622.

131 E. D. Bloch, D. Britt, C. Lee, C. J. Doonan, F. J. Uribe-Romo, H. Furukawa, J. R. Long and O. M. Yaghi, *J. Am. Chem. Soc.*, 2010, **132**, 14382–14384.

132 K. Manna, T. Zhang and W. Lin, *J. Am. Chem. Soc.*, 2014, **136**, 6566–6569.

133 Y. L. Wong, Y. Diao, J. He, M. Zeller and Z. Xu, *Inorg. Chem.*, 2019, **58**, 1462–1468.

134 M. I. Gonzalez, E. D. Bloch, J. A. Mason, S. J. Teat and J. R. Long, *Inorg. Chem.*, 2015, **54**, 2995–3005.

135 J. Becerra, D. T. Nguyen, V. N. Gopalakrishnan and T. O. Do, *ACS Appl. Energy Mater.*, 2020, **3**, 7659–7665.

136 A. Yazdi, A. Abo Markeb, L. Garzón-Tovar, J. Patarroyo, J. Moral-Vico, A. Alonso, A. Sánchez, N. Bastus, I. Imaz, X. Font, V. Puntes and D. Maspoch, *J. Mater. Chem. A*, 2017, **5**, 13966–13970.

137 P. Falcaro, R. Ricco, A. Yazdi, I. Imaz, S. Furukawa, D. Maspoch, R. Ameloot, J. D. Evans and C. J. Doonan, *Coord. Chem. Rev.*, 2016, **307**, 237–254.

138 P. Railey, Y. Song, T. Liu and Y. Li, *Mater. Res. Bull.*, 2017, **96**, 385–394.

139 B. An, L. Zeng, M. Jia, Z. Li, Z. Lin, Y. Song, Y. Zhou, J. Cheng, C. Wang and W. Lin, *J. Am. Chem. Soc.*, 2017, **139**, 17747–17750.

140 Y. Zhao, S. Zhang, M. Wang, J. Han, H. Wang, Z. Li and X. Liu, *Dalt. Trans.*, 2018, **47**, 4646–4652.

141 M. W. Zhang, M. T. Yang, S. Tong and K. Y. A. Lin, *Chemosphere*, 2018, **213**, 295–304.

142 F. R. Fortea-Pérez, M. Mon, J. Ferrando-Soria, M. Boronat, A. Leyva-Pérez, A. Corma, J. M. Herrera, D. Osadchii, J. Gascon, D. Armentano and E. Pardo, *Nat. Mater.*, 2017, **16**, 760–766.

143 M. A. Rivero-Crespo, M. Mon, J. Ferrando-Soria, C. W. Lopes, M. Boronat, A. Leyva-Pérez, A. Corma, J. C. Hernández-Garrido, M. López-Haro, J. J. Calvino, E. V. Ramos-Fernandez, D. Armentano and E. Pardo, *Angew. Chem., Int. Ed.*, 2018, **57**, 17094–17099.

144 M. Mon, M. A. Rivero-Crespo, J. Ferrando-Soria, A. Vidal-Moya, M. Boronat, A. Leyva-Pérez, A. Corma, J. C. Hernández-Garrido, M. López-Haro, J. J. Calvino, G. Ragazzon, A. Credi, D. Armentano and E. Pardo, *Angew. Chem., Int. Ed.*, 2018, **57**, 6186–6191.

145 M. Mon, R. Adam, J. Ferrando-Soria, A. Corma, D. Armentano, E. Pardo and A. Leyva-Pérez, *ACS Catal.*, 2018, **8**, 10401–10406.

146 R. Adam, M. Mon, R. Greco, L. H. G. Kalinke, A. Vidal-Moya, A. Fernandez, R. E. P. Winpenny, A. Domenech-Carbo, A. Leyva-Perez, D. Armentano, E. Pardo and J. Ferrando-Soria, *J. Am. Chem. Soc.*, 2019, **141**, 10350–10360.

147 M. Mon, J. Ferrando-Soria, T. Grancha, F. R. Fortea-Pérez, J. Gascon, A. Leyva-Pérez, D. Armentano and E. Pardo, *J. Am. Chem. Soc.*, 2016, **138**, 7864–7867.

148 W. M. Bloch, A. Burgun, C. J. Coghlan, R. Lee, M. L. Coote, C. J. Doonan and C. J. Sumby, *Nat. Chem.*, 2014, **6**, 906–912.

149 P. Van Der Sluis and A. L. Spek, *Acta Crystallogr. Sect. A*, 1990, **46**, 194–201.

150 G. M. J. Schmidt, *Pure Appl. Chem.*, 1971, **27**, 647–678.

151 R. Peralta, M. Huxley, R. Young, O. M. Linder-Patton, J. D. Evans, C. J. Doonan and C. J. Sumby, *Faraday Discuss.*, *Advance Article* (DOI:10.1039/d0fd00012d).

152 A. Burgun, C. J. Coghlan, D. M. Huang, W. Chen, S. Horike, S. Kitagawa, J. F. Alvino, G. F. Metha, C. J. Sumby and C. J. Doonan, *Angew. Chem., Int. Ed.*, 2017, **129**, 8532–8536.

153 R. A. Peralta, M. T. Huxley, J. D. Evans, T. Fallon, H. Cao, M. He, X. S. Zhao, S. Agnoli, C. J. Sumby and C. J. Doonan, *J. Am. Chem. Soc.*, 2020, **142**, 13533–13543.

154 C. Wang, B. An and W. Lin, *ACS Catal.*, 2019, **9**, 130–146.

155 R. J. Young, M. T. Huxley, E. Pardo, N. R. Champness, C. J. Sumby and C. J. Doonan, *Chem. Sci.*, 2020, **11**, 4031–4050.

156 H. Kim, S. Yang, S. R. Rao, S. Narayanan, E. A. Kapustin, H. Furukawa, A. S. Umans, O. M. Yaghi and E. N. Wang, *Science*, 2017, **356**, 430–434.

157 M. W. Logan, S. Langevin and Z. Xia, *Sci. Rep.*, 2020, **10**, 1–11.

158 D. DeSantis, J. A. Mason, B. D. James, C. Houchins, J. R. Long and M. Veenstra, *Energy and Fuels*, 2017, **31**, 2024–2032.

159 A. Schaate, P. Roy, A. Godt, J. Lippke, F. Waltz, M. Wiebcke and P. Behrens, *Chem. - A Eur. J.*, 2011, **17**, 6643–6651.

160 A. Sorrenti, L. Jones, S. Sevim, X. Cao, A. J. Demello, C. Martí-Gastaldo and J. Puigmartí-Luis, *J. Am. Chem. Soc.*, 2020, **142**, 9372–9381.

161 F. Banihashemi, G. Bu, A. Thaker, D. Williams, J. Y. S. Lin and B. L. Nannenga, *Ultramicroscopy*, 2020, **216**, 113048.

162 Z. Huang, E. S. Grape, J. Li, A. K. Inge and X. Zou, *Coord. Chem. Rev.*, 2021, **427**, 213583.

163 Z. Huang, T. Willhammar and X. Zou, *Chem. Sci.*, 2021, *Advance Article* (DOI:10.1039/D0SC05731B).

164 W. Xu, B. Tu, Q. Liu, Y. Shu, C. C. Liang, C. S. Diercks, O. M. Yaghi, Y. B. Zhang, H. Deng and Q. Li, *Nat. Rev. Mater.*, 2020, **5**, 764–779.

165 V. Guillerm and D. Maspoch, *J. Am. Chem. Soc.*, 2019, **141**, 16517–16538.

166 U. Fluch, B. D. McCarthy and S. Ott, *Dalt. Trans.*, 2019, **48**, 45–49.